Improving the Performance and Yield of Colloidal Quantum Dot Solar Cells through Electron Transport Layer Optimization

Dana Kachman,[1] Arlene Chiu,[1] Dhanvini Gudi,[1] Chengchangfeng Lu,[1] Eric Rong, [1] Sreyas Chintapalli,[1] Yida Lin,[1] Daniel Khurgin,[2] and Susanna M. Thon[1]

[1] Department of Electrical and Computer Engineering, Johns Hopkins University, Baltimore, Maryland, 21218, United States

[2] Department of Chemical and Biomolecular Engineering, University of California Los Angeles, Los Angeles, California, 90095, United States

***Abstract* — Colloidal quantum dots (CQDs) are promising materials for photovoltaic applications due to their solution processibility and size-dependent band gap tunability. The electron transport layer (ETL) is an important component of PbS CQD solar cells, and the quality of the zinc oxide nanoparticle (ZnO NP) ETL film significantly impacts both the power conversion efficiency (PCE) and fabrication yield of CQD solar cells. We report on multiple methods to improve the quality of ZnO NP ETL films and demonstrate increased PCE and device yield in standard CQD solar cells employing optimized ZnO NP films. We also discuss the application of these methods in an inverted CQD solar cell architecture.**

I. Introduction

Lead sulfide colloidal quantum dots (PbS CQDs) are of interest for photovoltaic applications due to their low-temperature synthesis, solution processability, and band gap tunability. These properties allow for many applications beyond those of traditional solar cells, such as in hybrid multijunction solar cells, flexible solar cells, and building-integrated photovoltaics. The maximum efficiency achieved in a PbS CQD solar cell is 15.4% [1], as compared to 26.7% for market-leading silicon solar cells [2]. While significant progress has been made in improving CQD solar cell performance, their efficiency needs to be further improved to make them a commercially viable technology. Additionally, further study is required to analyze and improve the yield of current fabrication techniques, where yield is defined as the percentage of working devices per fabrication batch. We have identified that many popular zinc oxide nanoparticle (ZnO NP) synthesis methods yield inconsistent results for the electron transport layer (ETL), frequently including a large percentage of shorted and low PCE devices. We report on two methods to decrease agglomeration during ZnO NP synthesis and improve the PCE and yield of CQD solar cells.

We also report on the applications of these methods in the optimization of an inverted CQD solar cell architecture. Currently, material properties of the hole transport layer (HTL) are also limiting device PCE [3], so developing an inverted CQD solar cell to facilitate the incorporation of novel materials as the HTL is an important goal. However, this architecture presents new fabrication challenges, as the ZnO NPs must be deposited on top of the CQD layer. We demonstrate approaches to overcome the damage to the CQD film and resulting shunting and decreased performance when depositing ZnO NPs onto a PbS CQD film.

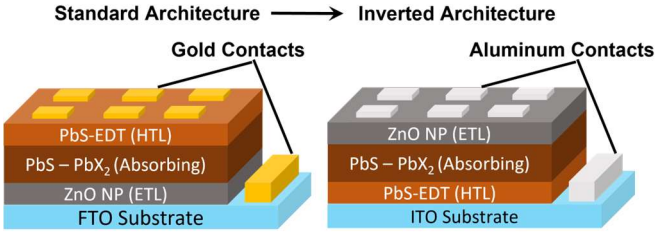

Fig. 1. Schematics of a standard (left) and an inverted (right) PbS CQD solar cell.

II. ETL Optimization In A Standard CQD Solar Cell

We optimized synthesis time as well as the final solvent in the ZnO synthesis method popularized by Chuang et al. [4] to improve PbS CQD solar cell device performance and yield.

A. Synthesis Parameter Optimization

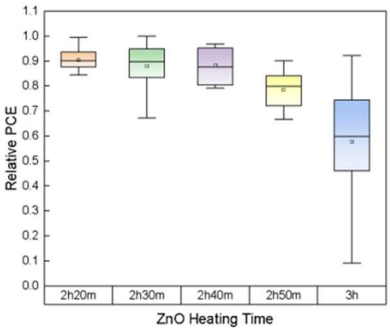

Fig. 2. PbS CQD solar cell PCE relative to the best performing device for ETLs made from ZnO NPs heated for different amounts of time. 9 devices were measured at each heating time.

We first optimized the heating time for the ZnO synthesis. To explore all common heating times [4]-[5], we varied the ZnO synthesis time from 2 hours and 20 minutes to 3 hours. We observed that shorter heating times yielded higher average PCE in devices, but the ZnO NPs were hard to redisperse in

2023 IEEE 50th Photovoltaic Specialists Conference (PVSC) | 978-1-6654-6059-0/23/$31.00 ©2023 IEEE | DOI: 10.1109/PVSC48320.2023.10359662

methanol, which is used as the washing solvent. We found the best trade off at 2 hours and 40 minutes of heating time. This allowed for reliable washing in methanol without a significant reduction of device PCE (fig. 2).

We also performed an optimization of the final ZnO dispersion solvent. Chuang et al. used pure chloroform for their final solvent, while Lan et al. added methanol to the final solvent in 2016 [4],[6]. Lan et al. found that the optimal ratio was 1:1 chloroform to methanol. This ratio results in minimal agglomeration, leading to better film morphology and ultimately improved device performance. Our results agreed well with this finding, and we additionally found that while higher chloroform-to-methanol ratios can produce high-performance devices, device fabrication yield was significantly better at a 1:1 ratio than at other ratios (fig. 3).

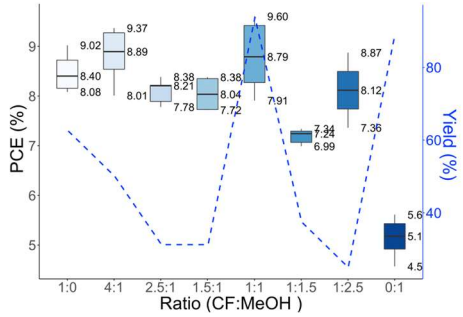

Fig. 3. Plots of the power conversion efficiency (PCE) of devices made with different ratios of chloroform (CF) and methanol (MeOH) for the final ZnO solution as well as the corresponding yield of working devices. 16 devices were measured at each ratio, except for the 0:1 ratio, for which 9 devices were measured.

III. ETL Optimization In An Inverted CQD Solar Cell

We next moved on to optimizing the performance of an inverted architecture PbS CQD solar cell. We chose to start with the method published by Ning et al. in 2018 [7], which uses the same ZnO film fabrication procedure discussed above, with minor modifications. For our devices, we used an amine mixture (10:3:2 butylamine: pentylamine: hexylamine) at a concentration of 300 mg/mL [8] for the PbS CQD absorbing layer.

A. SCAPS-1D Simulations

We studied the performance of inverted devices by conducting simulations using SCAPS-1D solar cell simulations [9]. We first directly inverted the solar cell structure, maintaining layer thicknesses and only changing the identity of the contacts. Our inverted devices use an ITO transparent contact and aluminum as the top contact, as seen in fig. 1. We found that directly inverting the CQD solar cell led to losses in both short circuit current density (Jsc) and open circuit voltage (Voc) (fig. 4). We attributed the drop in Jsc to non-optimized layer thicknesses. Since the *pn* junction is located at the absorbing layer/electron transport layer interface, it is further from the illumination side of the device compared to the standard architecture. We thus expected that a thinner hole transport layer and absorbing layer would be needed to optimize charge extraction within the device. We confirmed this by conducting SCAPS simulations to optimize over a range of HTL and absorbing layer thicknesses (fig. 4).

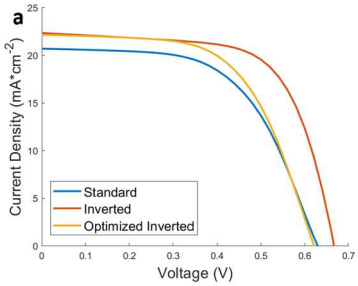

b

	Standard Architecture	Optimized Inverted Architecture	Inverted Architecture
Absorbing Layer thickness (nm)	400	350	400
HTL thickness (nm)	60	25	60
$J_{sc}\ \left(mA/cm^2\right)$	22.4	22.2	20.7
$V_{oc}\ (V)$	0.67	0.62	0.63
FF	0.66	0.59	0.57
$PCE(\%)$	9.78	8.13	7.49

Fig. 4. (a) JV curves for standard and inverted devices from SCAPS-1D simulations and (b) the corresponding device parameters. The inverted architecture was optimized by sweeping over a range of absorbing layer and hole transport layer thicknesses.

We saw significant improvement in the Jsc based on this optimization, but we still observed low Voc. Previous work on inverted devices has shown that the work function of the contacts has a significant impact on device performance [10], so we concluded that our current transparent contact did not have a sufficiently deep work function, which was limiting charge extraction from the hole transport layer. We confirmed this by conducting a SCAPS-1D simulation sweep of transparent contact work function, and we saw significant increases in the Voc as we increased the work function up to approximately 4.9 eV (fig. 5).

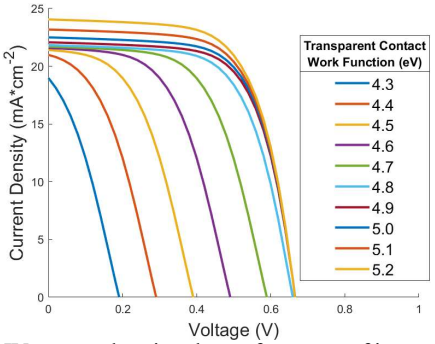

Fig. 5. JV curves showing the performance of inverted CQD solar cells with various work functions for the transparent contact, as indicated by the legend.

B. Experimental Results

We also experimentally fabricated inverted CQD solar cell devices. We developed two approaches to improve the performance of the devices. The first approach was developed to address the low fill factor seen in our initial devices. We hypothesized that the low fill factor was a result of shunts in the device due to cracks in the absorbing layer film. We further hypothesized that the ZnO film deposition could be partially dissolving the absorbing layer if the absorbing layer was not fully dry before ZnO deposition. To address this issue, we introduced an annealing step after depositing the absorbing layer and let the film dry for at least 24 hours in a glovebox before depositing the ZnO film. Using this approach, we saw significant increases in both fill factor and Jsc (fig. 6).

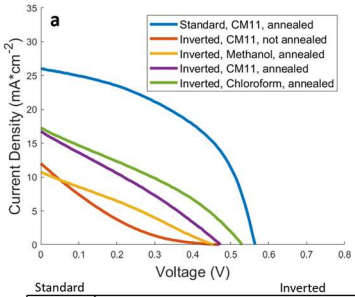

b

	Standard	Inverted			
ZnO Dispersion Solvent	**CM1:1**	**CM1:1**	**CM1:1 (No anneal)**	**Chloroform only**	**Methanol only**
$J_{sc}\ \left(mA/_{cm^2}\right)$	22.7	13.3	9.5	14.6	9.7
$V_{oc}\ (V)$	0.49	0.40	0.43	0.52	0.36
FF	0.42	0.28	0.15	0.29	0.29
$PCE(\%)$	5.1	1.5	0.6	2.2	1.0

Fig. 6. (a) JV curves and (b) solar cell parameters for experimentally fabricated inverted CQD solar cells. The data columns in (b) correspond to the blue, purple, orange, green, and yellow JV curves in (a), respectively.

We also conducted a solvent optimization study for the ZnO layer in an inverted device. We tested devices made with ZnO from just chloroform, just methanol, and a 1:1 chloroform and methanol solution. Our results show that using just chloroform significantly improved device performance, primarily through improved Voc. We are currently conducting further studies to determine the mechanism of Voc improvement and continue optimization of the inverted CQD solar cells to match performance in the standard architecture devices.

IV. Conclusion

We experimentally optimized both the heating time and final dispersion solvent for ZnO NPs used as the ETL for CQD solar cells. We showed that the fabrication yield of high-performance cells varies significantly as a function of both synthesis conditions. Device yield is an under-reported metric that will become increasingly important as CQD solar cells become commercially viable.

We additionally explored how these methods can be applied in an inverted CQD solar cell. We conducted SCAPS simulations to determine the optimal CQD layer thicknesses and determine the ideal work function for the transparent contact. Finally, we demonstrated two modifications to current fabrication techniques that improve the performance of inverted CQD solar cells, paving the way to further PCE improvements.

V. Acknowledgements

This work was funded by the National Science Foundation (DMR-1807342, ECCS- 1846239) and the US Department of Defense (W911NF2120213).

References

[1] C. Ding, D. Wang, D. Liu, H. Li, Y. Li, S. Hayase, T. Sogabe, T. Masuda, Y. Zhou, Y. Yao, Z. Zou, R. Wang and Q. Shen, "Over 15% Efficiency PbS Quantum-Dot Solar Cells by Synergistic Effects of Three Interface Engineering: Reducing Nonradiative Recombination and Balancing Charge Carrier Extraction," Adv.Energy Mater., vol. 12, pp. 2201676, 2022.

[2] M. Green, E. Dunlop, J. Hohl-Ebinger, M. Yoshita, N. Kopidakis and X. Hao, "Solar cell efficiency tables (version 57)," Prog Photovolt Res Appl, vol. 29, pp. 3-15, 2021.

[3] E. Rong, A. Chiu, C. Bambini, Y. Lin, C. Lu and S. M. Thon, "New Chalcogenide-Based Hole Transport Materials for Colloidal Quantum Dot Photovoltaics," in - 2021 IEEE 48th Photovoltaic Specialists Conference (PVSC), pp. 750, 2021.

[4] C.M. Chuang, P.R. Brown, V. Bulović and M.G. Bawendi, "Improved performance and stability in quantum dot solar cells through band alignment engineering," Nature Materials, vol. 13, pp. 796-801, 2014.

[5] Y. Wang, K. Lu, L. Han, Z. Liu, G. Shi, H. Fang, S. Chen, T. Wu, F. Yang, M. Gu, S. Zhou, X. Ling, X. Tang, J. Zheng, M.A. Loi and W. Ma, "In Situ Passivation for Efficient PbS Quantum Dot Solar Cells by Precursor Engineering," Adv Mater, vol. 30, pp. 1704871, 2018.

[6] X. Lan, O. Voznyy, A. Kiani, F.P. García de Arquer, A.S. Abbas, G. Kim, M. Liu, Z. Yang, G. Walters, J. Xu, M. Yuan, Z. Ning, F. Fan, P. Kanjanaboos, I. Kramer, D. Zhitomirsky, P. Lee, A. Perelgut, S. Hoogland and E.H. Sargent, "Passivation Using Molecular Halides Increases Quantum Dot Solar Cell Performance," Adv Mater, vol. 28, pp. 299-304, 2016.

[7] R. Wang, X. Wu, K. Xu, W. Zhou, Y. Shang, H. Tang, H. Chen and Z. Ning, "Highly Efficient Inverted Structural Quantum Dot Solar Cells," Adv Mater, vol. 30, pp. 1704882, 2018.

[8] J. Xu, O. Voznyy, M. Liu, A.R. Kirmani, G. Walters, R. Munir, M. Abdelsamie, A.H. Proppe, A. Sarkar, F.P. García de Arquer, M. Wei, B. Sun, M. Liu, O. Ouellette, R. Quintero-Bermudez, J. Li, J. Fan, L. Quan, P. Todorovic, H. Tan, S. Hoogland, S.O. Kelley, M. Stefik, A. Amassian and E.H. Sargent, "2D matrix engineering for homogeneous quantum dot coupling in photovoltaic solids," Nature Nanotechnology, vol. 13, pp. 456-462, 2018.

[9] M. Burgelman, P. Nollet and S. Degrave, "Modelling polycrystalline semiconductor solar cells," Thin Solid Films, vol. 361, pp. 527-532, 2000.

[10] G. Kim, B. Walker, H. Kim, J.Y. Kim, E.H. Sargent, J. Park and J.Y. Kim, "Inverted Colloidal Quantum Dot Solar Cells," Adv Mater, vol. 26, pp. 3321-3327, 2014.